Meteorol. Atmos. Phys. 44, 281–292 (1990)

Meteorology and Atmospheric Physics

551.515.7(57:59)

Academy of Meteorological Science, State Meteorological Administration, Beijing, China

Build-Up, Air Mass Transformation and Propagation of Siberian High and Its Relations to Cold Surge in East Asia

Ding Yihui

With 12 Figures

Received June 19, 1989
Revised November 22, 1989

Summary

The present paper discusses the build-up, the air mass transformation and the propagation of the Siberian high as well as its relations to the development of cold surges in East Asia. It has been found that (1) the genesis and development of the Siberian high result from the combined effects of the mass convergence at middle and upper-level and the radiative cooling; (2) the apparent transformation of the Siberian high over land is observed in winter, which is caused by the upward sensible heat and latent heat flux from the underlying surface; (3) the Siberian high and its attendant cold air outbreaks usually undergo a marked low-frequency, southward propagation with the period of 10–20 days; (4) activity of cold surge over the East China Sea and the South China Sea is closely related to the intensity of the Siberian high. The active cold surge occurs when the Siberian high is usually strong.

1. Introduction

The winter monsoon in East Asia is one of the most significant features of winter circulation over the northern hemisphere. It is closely related to cold air outbreaks over East Asia or activity of cold waves. The cold air flowing southward out of Siberian highs causes the intensification of the low-level northerly wind or northeasterly wind, thus producing cold surges. When the cold surge rapidly propagates southward down to the near-equatorial region, it may enhance convection and precipitation there. Subsequently, the released condensation heating may exert a significant effect on atmospheric circulation over East Asia as well as the northern hemisphere through the enhanced Hadley and Walker circulations. Thus, the winter monsoon in East Asia involves with numerous important weather events, mainly including: (1) the large-scale circulation and the regional conditions of development of Siberian highs; (2) the transformation of cold air at land and oceanic surfaces; (3) the development and southward propagation of cold surges; and (4) the planetary-scale effect of the winter monsoon. In the recent decade, a number of investigators have studied the problems (3) and (4) as well as air mass transformation over the ocean (Chang and Lau, 1980; Lau, 1982; Lim and Chang, 1981; Ninomiya, 1975, 1977; Nitta and So, 1980; Pan and Zhou, 1985). However, very few works have been done on the early stage of the development of the winter monsoon.

Recently, Ding and Krishnamurti (1987) have studied the heat budget of the Siberian high and the winter monsoon, pointing out that strong radiative cooling and large-scale descending motion (with large-scale mass convergence over the upper and middle troposphere and divergence over the lower troposphere) contributes to the build-up of the Siberian high. Heating in the upper troposphere due to subgrid-scale sensible heat transfer is also an important factor in the maintenance of mass convergence in the upper troposphere

through enhancement of the warm upper tropospheric anticyclone lying over the Siberian high.

The present paper is a further study of this problem. We shall first analyse the dynamic structure, and budgets of vorticity and heat in Section 2, thus gaining an insight into the physical processes leading to the build-up of the Siberian high. Then, in order to understand the air mass transformation over land of the Siberian high, the sensible and latent heat flux from the surface was directly estimated by use of similarity theory. In Section 4, we shall briefly discuss the southward propagation of the high, as a low-frequency oscillation. Finally, we shall address the relationship between the Siberian high and the development of the cold surge.

2. Case Selection and Data Sets

As indicated by Ding and Krishnamurti (1987), the Northwest (NW) track of Siberian highs is the most frequently observed. This track accounts for nearly 64% of all the paths of Siberian highs investigated by them. The same criteria as those adopted in Ding and Krishnamurti (1987) are used to select the cases of Siberian highs from ECMWF data sets for four winters (December through February) of 1980–1983. Alltogether, five cases of southeastward moving (NW track) intense Siberian highs were chosen for dynamic study of structure of these highs (Table 1).

Along the NW track of Siberian highs, the four subregions (Box 1– 4) were defined for calculating the area-averaged variables and budgets of heat and vorticity. Box 1 (80–120° E, 42.5–57.5° N) represents the origin region of Siberian highs where they build up. The regions represented by Box 2, Boxes 3 and 4 are fully same as those defined in Ding and Krishnamurti (1987). They nearly cover North China, East China and the northern part of South China, and the East China Sea, respectively.

Table 1. *The Selected Cases of Siberian Highs During the Four Winters of 1980–1983*

Case	Date	Initial stage	Mature stage
1	Jan. 26–30, 1980	Jan. 26, 1980	Jan. 27–29, 1980
2	Jan. 21–28, 1981	Jan. 21, 1981	Jan. 22–28, 1981
3	Feb. 23–28, 1981	Feb. 23–24, 1981	Feb. 25–27, 1981
4	Dec. 2–5, 1982	Dec. 2, 1982	Dec. 3–5, 1982
5	Jan. 4–8, 1983	Jan. 4–5, 1983	Jan. 6–7, 1983

In order to better understand the difference in dynamic structure of Siberian highs for the different stage of devleopment, two stages were divided for Box 1, namely, the initial stage and the mature stage. The former is defined as initially developing Siberian highs with the surface central pressure lower than 1 045 hPa, while the latter is defined as intense Siberian highs with a surface central pressure greater than 1 045 hPa (see Table 1).

The estimates of surface sensible and latent heat fluxes for Boxes 2 and 3 were carried out directly by use of station data within these regions. Each box includes 6–8 surface stations and 4–6 upper-air radiosonde stations that are generally located around the central part of Siberian highs. The four times–daily surface observations (0200, 0800, 1400, 2000 hr for Beijing local time) were used to estimate the surface fluxes and their diurnal variations. Surface observations include surface air temperature, dew-point temperature, wind vector, station pressure and soil moisture.

In Section 6, a longer period data set of ECMWF for 1979–1984 were used for a statistical study of cold surge in East Asia. First, the multi-year climatological averages were computed and then the averages of individual year and inter-annual variability of cold surge were further computed.

3. Build-Up of the Siberian High

The Siberian high usually has very high surface pressure values, generally at the range of 1 050–1 070 hPa, even in excess of 1 080 hPa in the extreme case. This increase of surface pressure by 50–70 hPa in a few days indicates the presence of strong net mass convergence in the region of the high, which may be caused by dynamic and/or thermal factors. For this purpose, a study of the dynamic structure and budgets of vorticity and heat of the Siberian high has been made to explore dynamic and thermal factor critical for local build-up of the high. At the initial stage of the formation of the Siberian high, the positive vorticity dominates the region of the high in the troposphere (Fig. 1). There is the convergence at low-level and high-level, respectively, with the divergence in between (Fig. 2). Correspondingly, there is the up-

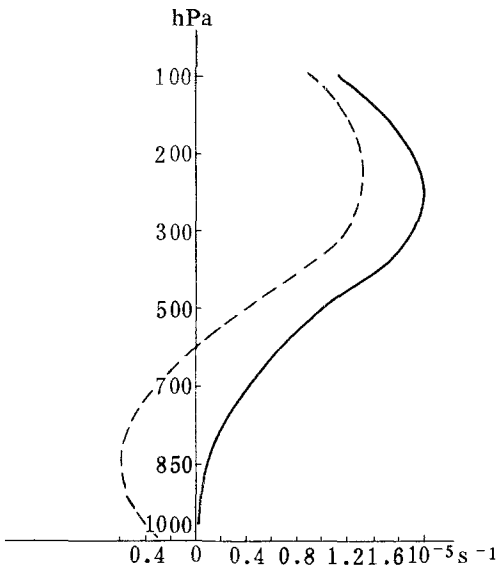

Fig. 1. The profiles of mean vorticity for the Siberian high, averaged for five cases in the domain of 40–60° N, 77.5–122.5° E. The full line denotes the curve for the initial stage and the dashed line the curve for the mature stage. Unit: $10^{-5}s^{-1}$

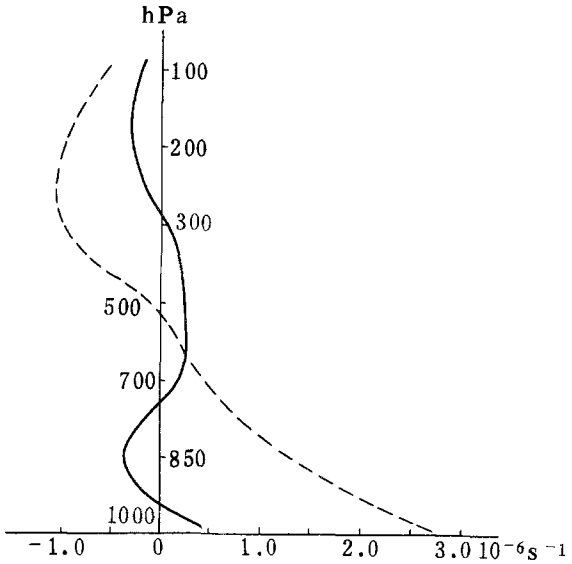

Fig. 2. Same as Fig. 1, but for the divergence

ward motion in the layer below 700 hPa and the downward motion above 700 hPa (Fig. 3). In contrast, at the mature stage of the Siberian high, the significant negative vorticity and strong divergent airflows are observed in the lower and middle troposphere while there is positive vorticity and convergent airflows in the upper troposphere. The downward motion occurs in the whole layer of troposphere (Fig. 3). This rapid change in dynamic structure of the Siberian high shows that its build-up is closely related to significant mass convergence in the upper troposphere, which is a necessary requirement for rapid increase in surface pressure.

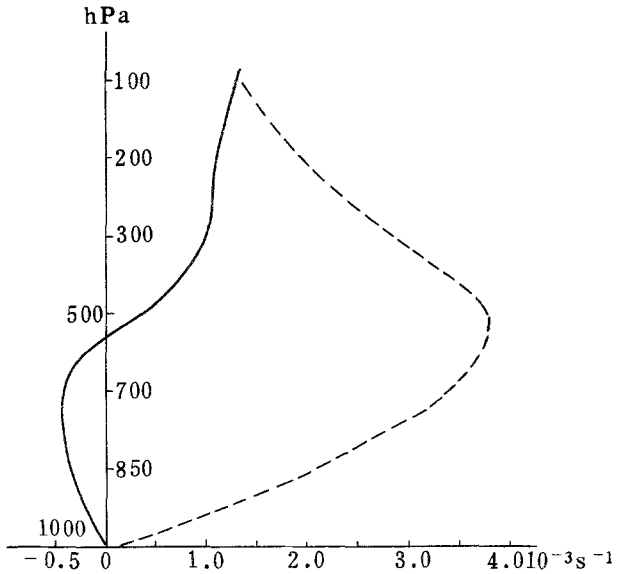

Fig. 3. Same as Fig. 1, but for the vertical velocity ω ($=dp/dt$). Unit: 10^{-3} hpas^{-1}

In order to further understand the physical implication of the above-described vorticity profiles, the vorticity equation is used to make a diagnostic analysis of the relative contribution of its various terms to the composite vorticity field,

$$\underset{(G)}{\frac{\partial \zeta}{\partial t}} = \underset{(A)}{-\mathbb{V}\cdot\nabla(\zeta+f)} \underset{(B)}{-\omega\frac{\partial \zeta}{\partial p}} \underset{(C)}{-(\zeta+f)\nabla\cdot\mathbb{V}} \underset{(D)}{-\mathbb{K}\cdot\nabla\omega\times\frac{\partial \mathbb{V}}{\partial p}} + \mathrm{R} \qquad (1)$$

Table 2 is the computed results averaged for five cases of the Siberian high. It can be seen that at the initial stage, the local change of the relative vorticity is positive in almost the whole troposphere, except for 1 000 hPa. This increase in the vorticiy is mainly caused by the advection of the vorticity (A), especially in the middle and upper troposphere. The divergence term (C) also makes some contribution, especially at low-level where it produces the positive vorticity. At the mature stage, however, the local change of the vorticity is negative in the whole troposphere, indicating the generation of the anticyclonic vorticity. This is fully consistent with the change of the relative vorticity, as shown in Fig. 1. The generation and

Table 2. *The Estimate of Various Terms of the Vorticity Equation* (1)

Level (hPa)	Initial stage						Mature stage					
	G	A	B	C	D	R	G	A	B	C	D	R
100	0.1	0.3	−0.1	0.2	−0.0	−0.3	−0.2	−0.7	−0.0	0.8	−0.0	−0.3
200	0.6	0.8	−0.0	0.5	−0.0	−0.6	−0.3	−1.8	0.0	1.4	0.0	0.1
300	0.8	1.3	0.1	−0.0	−0.0	−0.5	−0.4	−2.4	0.1	1.5	−0.1	0.5
500	0.5	0.9	0.2	−0.3	−0.1	−0.3	−0.4	−0.8	0.3	0.2	−0.2	0.1
700	0.2	0.7	0.1	−0.3	−0.1	−0.3	−0.4	0.2	0.2	−0.4	−0.1	−0.2
850	0.1	−0.1	−0.0	1.1	0.1	−0.9	−0.3	−0.1	−0.0	−1.0	0.1	0.7
1 000	−0.1	−0.4	0.0	0.1	−0.0	0.2	−0.1	−0.2	−0.0	−2.8	0.0	2.9

intensification of the negative vorticity in the Siberian high mainly results from the effects of the advection of the negative vorticity in the middle and upper troposphere and divergence term (convergence). At low-level, the divergence term (divergence) is the major factor for the generation of the negative vorticity. In general, the twisting term (D) is of minor importance. The residual term (R), including the friction and other effects, is the most significant near the surface, possibly indicating the importance of friction effect. This result is consistent with the patterns of large-scale airflows, because the advection of negative vorticity mainly occurs over the area in advance of the upper ridge and in rear of the upper trough, where the surface Siberian high is usually observed to develop rapidly. Dallavalle and Bosart (1975) previously studied the anticyclogenesis over North America and obtained a similar result. They pointed out that in the middle and upper troposphere, vorticity advection is most important in causing anticyclonic tendencies over and downwind of the surface anticylone. In contrast, divergence usually dominates in producing similar tendencies in the lower troposphere over the surface high.

The advection of negative vorticity in the middle and upper troposphere may cause the upper-level convergence. As an approximation, the equation of vorticity may be simplified as the following form, with neglecting the tendency term, twisting term and friction term:

$$\mathbb{V}\cdot\nabla(\zeta+f)\approx-(f+\zeta)\nabla\cdot\mathbb{V} \tag{2}$$

This equation is generally believed to be applicable in the middle and upper troposphere. For the advection of negative vorticity, $\mathbb{V}\cdot\nabla(\zeta+f)>0$, therefore, $\nabla\cdot\mathbb{V}<0$, i.e., there is the mass convergence in the upper troposphere. This fact also indicates the major importance of upper-level advective process for triggering and development of the Siberian high.

On the other hand, the heat budget of the Siberian high was estimated via budget calculation. The apparent heat source (Q_1) was calculated from large-scale variables according to the following equations:

$$Q_1 = Cp\left[\frac{\partial\theta}{\partial t}+\mathbb{V}\cdot\nabla\theta+\omega\frac{\partial\theta}{\partial p}\right]\left[\frac{p}{p_0}\right]^k \tag{3}$$

where θ is the potential temperature; ω the vertical velocity in p-coordinates, $k=R/Cp$ with R and Cp being the gas constant and the specific heat of dry air at constant pressure respectively; $p_0=1\,000$ hPa.

At the mature stages, there is a deep layer of cooling (Fig. 4), with the maximum cooling found in the lower and middle troposphere. This result has further documented the findings made previously by Ding and Krishnamurti (1987). But, at the initial stage, the profile of Q_1 is considerably different, with cooling observed only in layers below 850 hPa and above 500 hPa. The middle-level heating is obvious and may be associated with the condensational process in the high. The existence of upwarde motion below 550 hPa may lend some support to this inference. For the diabatic cooling, it consists of three components in the following thermodynamic equation:

$$\frac{Q_1}{C_p}=\left[\frac{\partial\theta}{\partial t}+\mathbb{V}\cdot\nabla\theta+\omega\frac{\partial\theta}{\partial p}\right]\left[\frac{p}{p_0}\right]^k = \frac{Q_R}{C_p}+\frac{Q_c}{C_p}+\frac{Q_s}{C_p} \tag{4}$$

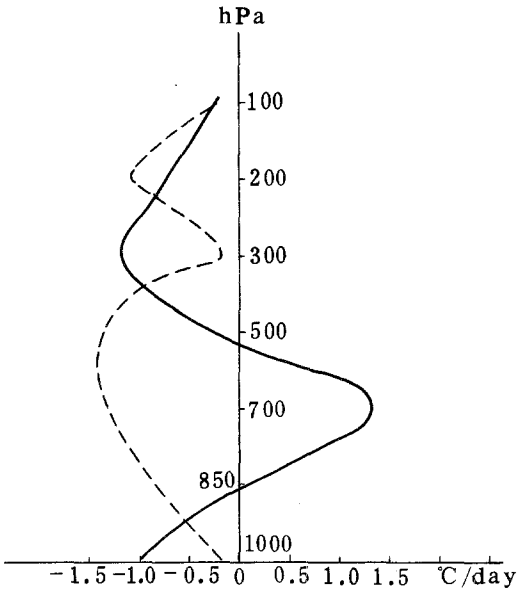

Fig. 4. Same as Fig. 1, but for the vertical profiles of area-averaged apparent heat source (Q_1). Unit: °C/day

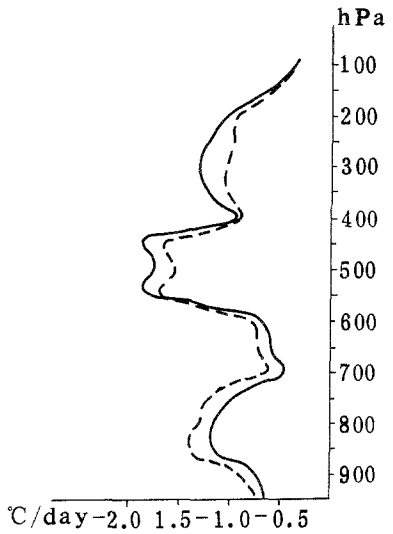

Fig. 5. Same as Fig. 1, but for the vertical profiles of area-averaged, long-wave radiative cooling rate. Unit: °C/day

where Q_c is the net condensation heating rate. Under the condition of the winter Siberian high, this component is negligibly small, especially at its mature stage. Q_s is the sensible heating which is mainly significant at low-level and near the tropopause (Ding and Krishnamurti, 1987). Therefore, for most of the tropospheric atmosphere, the component of the long-wave radiation Q_R (in this case solar radiation may be neglected because of late local time) may make a major contribution to diabatic heating. An attempt of direct estimate of this component was made.

The calculation of radiative fluxes is based on Yang and Krishnamurti (1981). A series of tests were performed to test the validity of the radiation scheme. Overall the results show that long-wave radiative fluxes computed by the emissivity method with a fine vertical resolution (50 hPa) were in reasonable agreement with the observations.

Figure 5 shows the profiles of Q_R for the initial and mature stages. It may be noted that these two curves are not considerably different, except for some magnitude of cooling rate. If one compares the Q_R profile at the mature stage with the corresponding Q_1 profile in Fig. 4, it can be found that both is nearly similar, indicating the maximum contribution of long-wave radiation to diabatic cooling at this stage. However, for the initial stage, this condition is not true. The heat budget might have a more complex picture which will not be addressed here. In response to the diabatic cooling, the downward motion in the deep layer of the troposphere can be induced, thus leading to the mass convergence in the middle and upper troposphere and the divergence in the lower troposphere. This condition is favorable to the development and the intensification of the Siberian high. Therefore, with combined consideration of the result derived from the analysis of the budget of vorticity, one may suggest that the genesis and development of the Siberian high results from the combined effects of the mass convergence at middle and upper level and the advection of the negative vorticity as well as local thermal cooling. Note that, in the present study, heating in the upper troposphere due to subgrid-scale sensible heat transfer, which may be an important factor in the maintenance of mass convergence in the upper troposphere through enhancement of the warm upper-tropospheric anticyclone lying over the Siberian high (Ding and Krishnamurti, 1987) is nonexistent (see Fig. 4). Compared to previous studies of anticyclogenes is the physical mechanism indicated here is at a certain degree different from the anticyclogenesis in Alaska (Bodurtha, 1952) which is caused by strong warm air advection prior to and during the period of anticylcogenesis in the low and middle troposphere, west of the location of anticyclogenesis, and the subsequent strong cold-air advection at 200 hPa over the region of anticyclogenesis in Alaska.

4. The Transformation of the Siberian High over Land

The cold high, once it moves away its source region, will undergo a considerable transformation due to the upward subgrid scale sensible and latent heat flux from the land surface. Through this process, the dynamic and thermal characteristics of the polar continental air mass associated with the Siberian high may be modified. Numerous works have delt with the transformation problem of cold air mass over the warm oceanic area, finding that this transformation process through the sensible heat and latent heat flux is particularly significant over the East China Sea. The studies for AMTEX' 74 and 75 indicated that during outbreak of cold air, the total heat flux from the Kuroshio warm current to the atmosphere (sensible heat flux plus latent heat flux) amounted to 800 W/m^2 over the land in East Asia. The cold air actually also undergoes a considerasble transformation process (Ding and Krishnamurti, 1987). The diabatic heating from the underlying surface commences shortly after it moves away from its source region and arrives in the Mongolian area and northern China. As the cold air further flows southward, this low-level heating becomes more significant and the depth of heating layer also increases, which may extend up to 700 hPa in eastern China. When the high arrives at lower latitudes, the heating due to condensation in the lower troposphere further enhances the transformation process of the cold high. Figure 6 shows variations of area-averaged temperature profiles in the cold high as it arrives in the different areas. In the source region (Box 1), there is a strong temperature inversion layer below 800 hPa. As the cold high moves southward, the inversion layer gradually weakens and disappears. In northern China (Box 2), it can not be detected. But, in eastern China (Box 3), a weak inversion or isothermal layer is reestablished in the middle troposphere that may be mainly caused by the strong dynamic descending motion in the high (Ding and Krishnamurti, 1987). Accompanying the evolution of the inversion layer, the temperature in the whole troposphere, especially in the lower troposphere, markedly enhances, thus leading to a gradual transformation from the deep, continental air mass into the warm oceanic air mass. The increase in the mean temperature near the surface and in the upper troposphere amounts to about 30 °C and 20 °C, respectively. The evolutive process of profiles of specific humidity is broadly similar to that of temperature profiles (Fig. 7). The moisture in the cold high rapidly increases as it moves southward, especially in the lower and middle troposphere. It is worthy to note that the increase of moisture from Box 2 to 3 below 700 hPa is quite marked, almost equal to the magnitude of increase of moisture over the ocean (from Box 3 to 4). This fact indicates the great importance of the variations of moisture field for the transformation of the cold high.

As previously indicated, the transformation of the cold high is mainly caused by the sensible

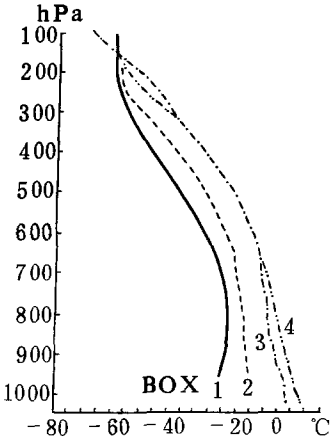

Fig. 6. The variations of area-averaged temperature profiles in the cold high as it arrives in the different areas. Box *1* the source region (the central and eastern Siberia), Box *2* North China, Box *3* the eastern China, and Box *4* the East China Sea. Five cases of the Siberian high were used to obtain these mean temperature profiles. Unit: °C

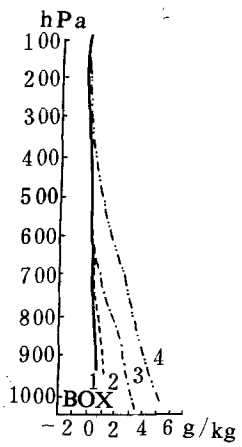

Fig. 7. Same as Fig. 6, but for the profiles of specific humidity. Unit: g kg^{-1}

heating and latent heating from the underlying surface. Based on the study of heat budget of 19 strong Siberian highs, Ding and Krishnamurti (1987) pointed out that the heating rate from the land surface (114 W/m^2) is about half or one third of that over the ocean (256–442 W/m^2). But, their estimate was based on the budget calculation method, i.e., residual method. Some computational errors could be included in the results. Now, the direct estimate of heat flux from the land surface for the different regions the Siberian high traverses has been attempted.

In order to take into account the effect of atmospheric stratification, the surface sensible heat (fh) and latent heat flux (fq) were estimated by use of similarity theory:

$$fh = \rho_s C_h C_p (T_{z_0} - T_s) |\mathbb{V}_s| \tag{5}$$

$$fq = \rho_s C_h L (q_{z_0} - q_s) |\mathbb{V}_s| \tag{6}$$

where ρ_s, T_s, $\mathbb{V}_s$, and q_s represent the near-surface air density, temperature, wind vector and specific humidity, respectively. T_{z_0} and q_{z_0} are the temperature and specific humidity at roughness height z_0 which is set to be 0.1 m, respectively.

$$T_{z_0} = T_G + 0.0096 (\theta^*/k) (u^* z_0/\gamma)^{0.45} \tag{7}$$

$$q_{z_0} = q_{sat}(T_{z_0}) RH \tag{8}$$

where T_G is the soil temperature at 0 cm, $\gamma = 1.5 * 10^{-5}$ m^2 s^{-1}, $u^* = |\overline{w'u'}|^{1/2}$, $\theta^* = -\overline{w'\theta'}/u^*$, RH is the relative humidity at z_0 and q_{sat} is the saturation specific humidity at T_0.

$$C_h = \{[k^2/(\ln z/z_0)]/R\} F_h \tag{9}$$

where k is the Von Karman constant, z is taken as 10 m, and R, the ratio of drag coefficient for momentum and that for heat under the neutral condition, is taken to be 0.74 (Businger et al., 1971), and

$$F_h = \begin{cases} 1 - bRib/(1 + C|Rib|^{1/2}) & \text{unstable} \\ 1/(1 + b' Rib)^2 & \text{stable} \end{cases} \tag{10}$$

where $Rib = gz[\theta(z) - \theta(z_0)]/\bar{\theta}\ u^2$, bulk Richardson number, $b = 2b' = 9.4$, $c = c^* a^2 b (z/z_0)^{1/2}$, $c^* = 5.3$ and $a^2 = k/(\ln z/\ln z_0)$.

The above described computational procedure is in many ways similar to the one suggested by Louis (1979).

Table 3 summarizes the computational results for Boxes 2 and 3 where major air masses transformation occurs. From the dially mean values,

Table 3. *The Mean Sensible Heat and Latent Heat Fluxes at the Land Surface in Winter, Averaged for Five Cases of Cold Waves*

Heat flux	Region	0200 (local time)	0800	1400	2000	daily mean
Sensible heat flux	Box 2	−18	−6	266	−12	57
	Box 3	−7	9	263	−8	49
Latent heat flux	Box 2	−3	−1	78	−3	18
	Box 3	−6	5	148	−7	35
Total heat flux	Box 2	−21	−7	344	−15	75
	Box 3	−13	14	351	−15	84
Bowen ratio	Box 2	6.0	6.0	3.4	1.8	3.2
	Box 3	1.2	1.8	1.4	0.5	1.4

the total heat flux in Boxes 2 and 3 is 84 W/m^2 and 75 W/m^2, respectively, with the sensible heating to make the major contribution (see Bowen ratio). These values of heat flux are slightly smaller than those obtained by Ding and Krishnamurti (1987), but they are nearly the same in the order of magnitude. Therefore, their heating effect on the cold high from the land surface can not be neglected. From Table 3, it is also seen that the heat flux assumes an obvious diurnal variation, with the maximum upward heat flux observed at 1400 (Beijing local time) and very weak heat flux (generally downward) at the other observation times.

5. The Southward Propagation of the Siberian High

The Siberian high and its associated winter monsoons usually show a marked low-frequency meridional movement (Lau and Lau, 1984; Pan and Zhou, 1985). These low-frequency perturbations with time scale between 10 and 30 days tend to migrate toward the subtropical Pacific, mostly accomplished by successive development of new centers downstream primary disturbance located over the western Pacific. Here, the further evidence will be presented to document low-frequency mode of meridional propagation of the winter monsoon. Figure 8 is x–t diagrams of Q_1, showing the temporal evolution of heat sources and sinks along the trajectory of cold air outbreaks at 700 hPa and 300 hPa, respectively. The selection of the time period from January 16 to February 15, 1981 covers the period of the vigorous cold air outbreaks.

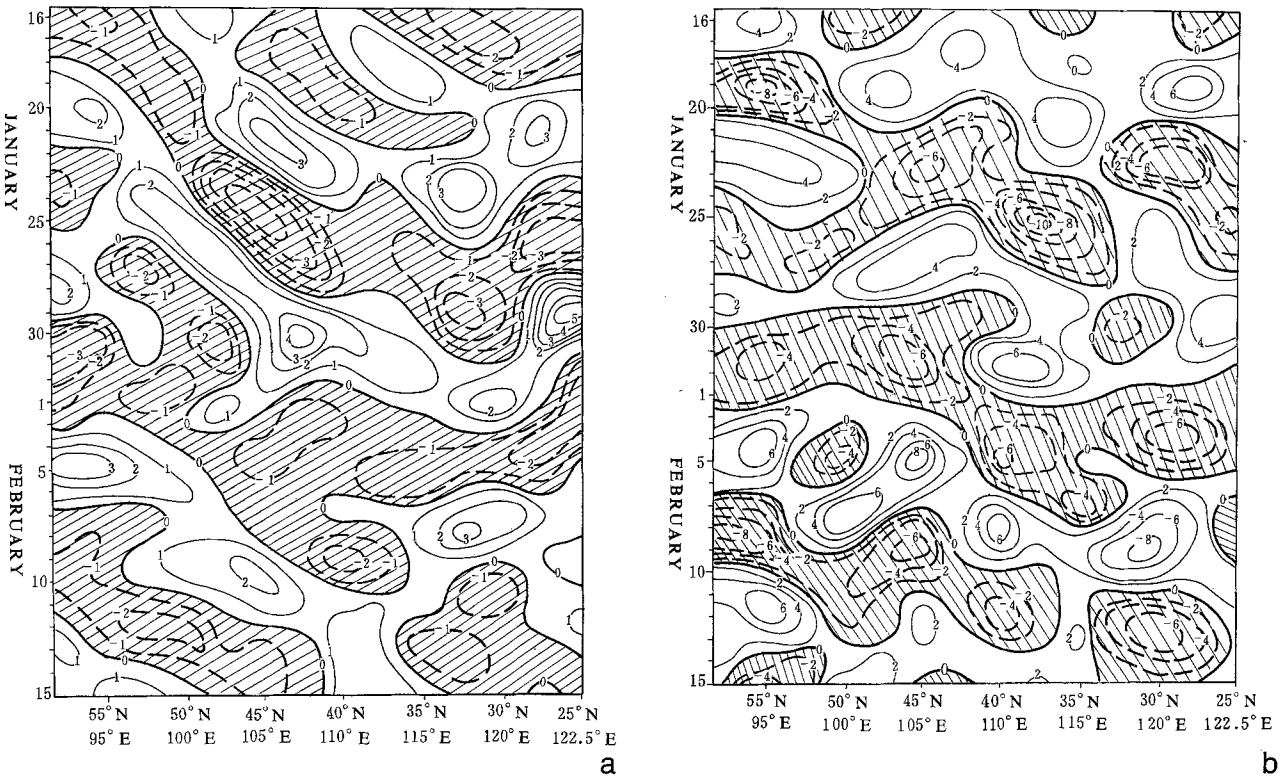

Fig. 8. x-t charts of lwo pass filtered apparent heat source Q_1 at 700 hPa (a) and 300 hPa (b) during the time period from January 15 to February 15, 1981. Negative area is shaded. Solid lines denote the positive (heating) Q_1 and dashed lines the negative (cooling) Q_1. Unit: °C/day. Abscissa is taken along the trajectory of the cold air outbreaks

First, the linear seasonal trend was removed from the once-daily Q_1 field. A time filter was next applied to the above fields of Q_1 at 700 hPa and 300 hPa, respectively, in order to obtain a smoothed distribution. From Fig. 8, one notes that roughly three cold air outbreaks propagate from their source region to the coastal area of southern China in a period of one month. The strongest episode, among these, is from January 21–29, 1981. The propagation of heat sources and sinks from NW to SE along the trajectory at 300 hPa appears to precede a corresponding propagation at the 700 hPa by almost 1–3 days. This southeastward propagation of Q_1 toward lower latitudes with the period of 10–20 days is closely related to the cold air outbreaks of East Asia. As a component of variations of the large-scale circulation features, the cold air outbreaks should be closely related to the low-frequency movement of trough and ridges at middle and high latitudes. Therefore, the low-frequency mode of the southward propagation of the winter monsoon actually reflects the characteristics of low-frequency oscillation systems at middle and high latitudes and their effect on the circulation condition at low-latitude (Krishnamurti and Gadgil, 1985).

6. Cold Surge in East Asia and Its Relationship to the Siberian High

When the winter monsoon arrives in southern China, the South China Sea and the tropical West Pacific, it can further intensify and usually becomes the prevailing northeasterly winds at low-level. This low-level northerly or northeasterly winds are so-called cold surges, and their intensity is defined with activity index of cold surge (Chang and Lau, 1980). Here, the north wind with wind speed greater than 5 m/s in magnitude and persistent for two days is defined as cold surge. This definition is more or less arbitrary, but it is deemed that the results obtained will not significantly differ from those based on greater north wind speed to define cold surge (Chang and Lau, 1980). Figure 9 is the mean distribution of frequency of occurrence of north wind greater than 5 m/s at 1 000

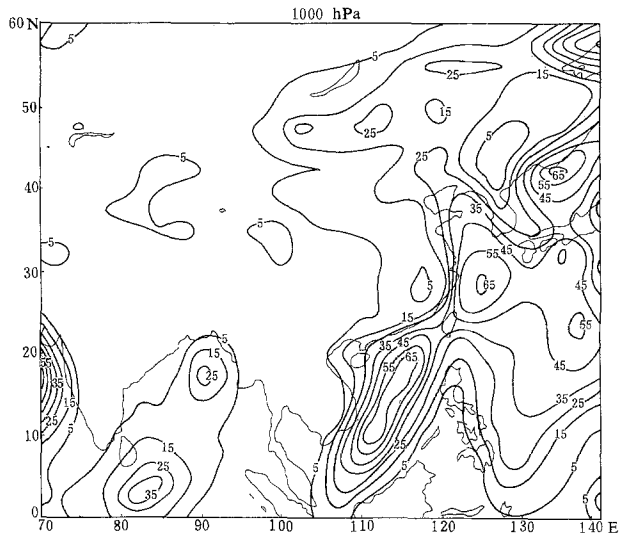

a

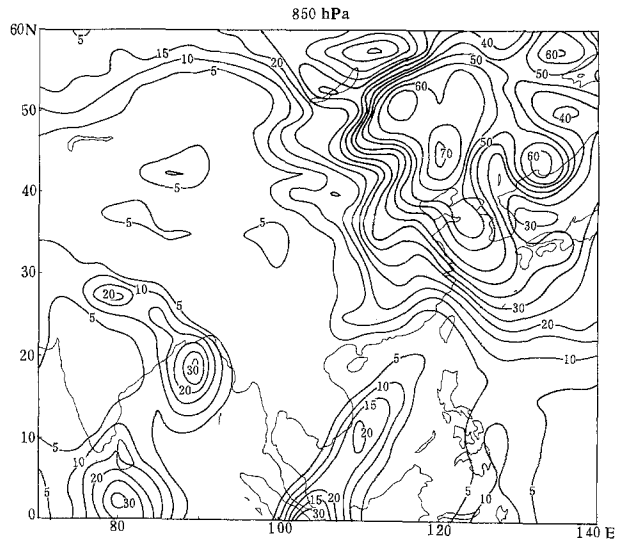

b

Fig. 9. The mean distribution of frequency of occurrence of north wind ($Vs<0$) greater than $5\,ms^{-1}$ in magnitude for five winters (December–February) of 1979–1984. (a) 1 000 hPa and (b) 850 hPa

and 850 hPa, showing clearly the climatological locations of cold surge. Near the surface (1 000 hPa), the maximum frequency of cold surge (65%) occurs over the South China Sea. Another region of high frequency is located over the oceanic area to the east of the Philippines, but the frequency of the latter only accounts for half of that of the former. Therefore, the strongest cold surge near the surface is observed over the South China Sea. This conclusion is consistent with that obtained by the study of cold surge for individual year. At 850 hPa, the frequency of occurrence of cold surge over the South China Sea significantly decreases, being half of the frequency near the surface, and the maximum of frequency shifts toward Malaysia and Indonesia. The cold surge over the West Pacific almost disappears (10%). Note that the cold surges over the South China Sea and over the West Pacific nearly completely disappears at 700 hPa (not shown). From the above discussion, the cold surge is a phenomenon in the shallow layer below 700 hPa. In short, it most frequently occurs near the surface and has the maximum wind speed. Then, the intensity and frequency of cold surge both decreases with height, and almost can not be detectable at 700 hPa.

It is very interesting to compare the patterns of cold surge with the mean winter weather maps at 1 000 and 700 hPa (Fig. 10). At 1 000 hPa, there is a huge cold high, with its center located over the central and eastern Siberia and Mongolia. Its high pressure extends southward all the way down to the equatorial region (around 10° N). There is the significant pressure gradient over the East China Sea and the South China Sea where the most vigorous cold surge exists. At 850 hPa, one can only see the remnants of the cold high in the south, implying that the cold high that spreads down to the lower latitude is very shallow, mainly confined in the layer below 850 hPa. At 700 hPa, the synoptic situation in East Asia is quite different from that at lower level in that the basic aircurrents go around the Tibetan Plateau and split into two

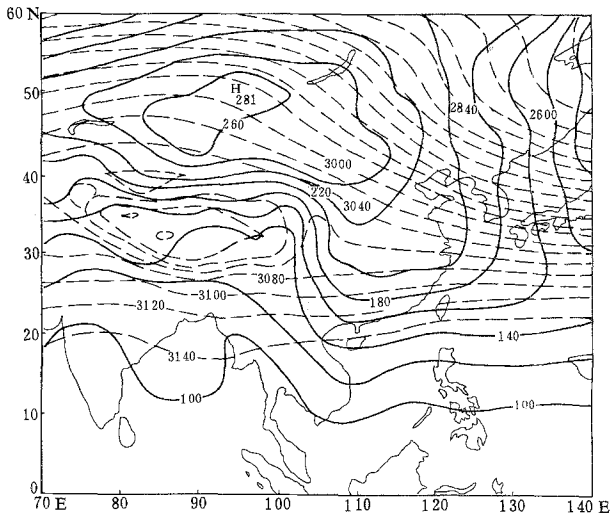

Fig. 10. 5-year (1979–1984) mean winter weather maps at 1 000 hPa (solid lines) and 700 hPa (dashed lines). Unit of geopotential height: decameter

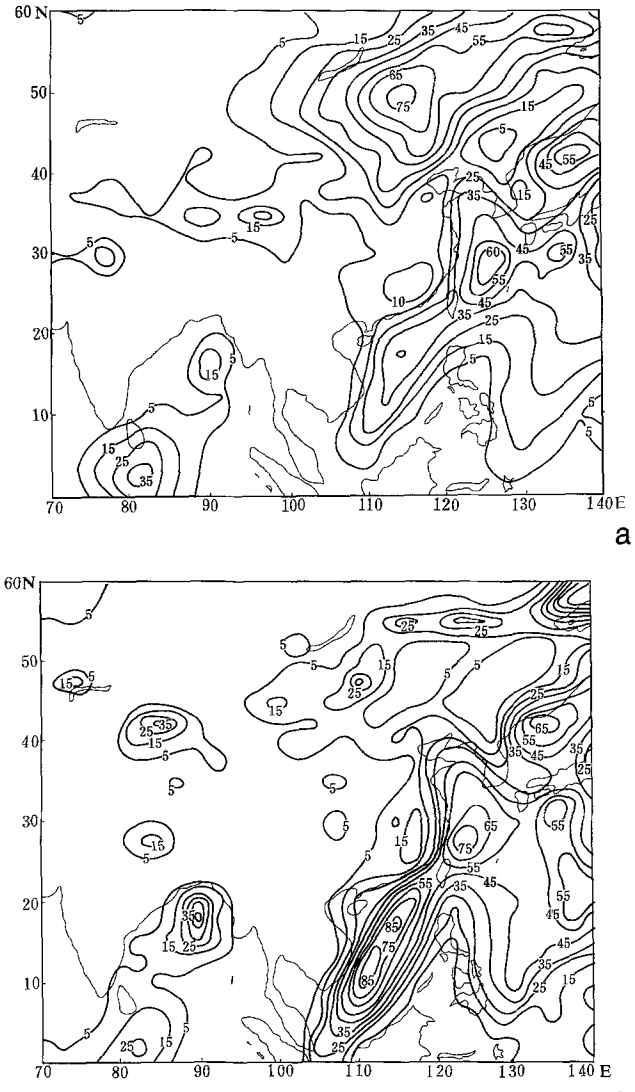

Fig. 11. Distributions of occurrence frequency of northerly wind greater than $5\,ms^{-1}$ in magnitude for the winter of 1979–1980 (a) and 1983–1984 (b) at 1 000 hPa

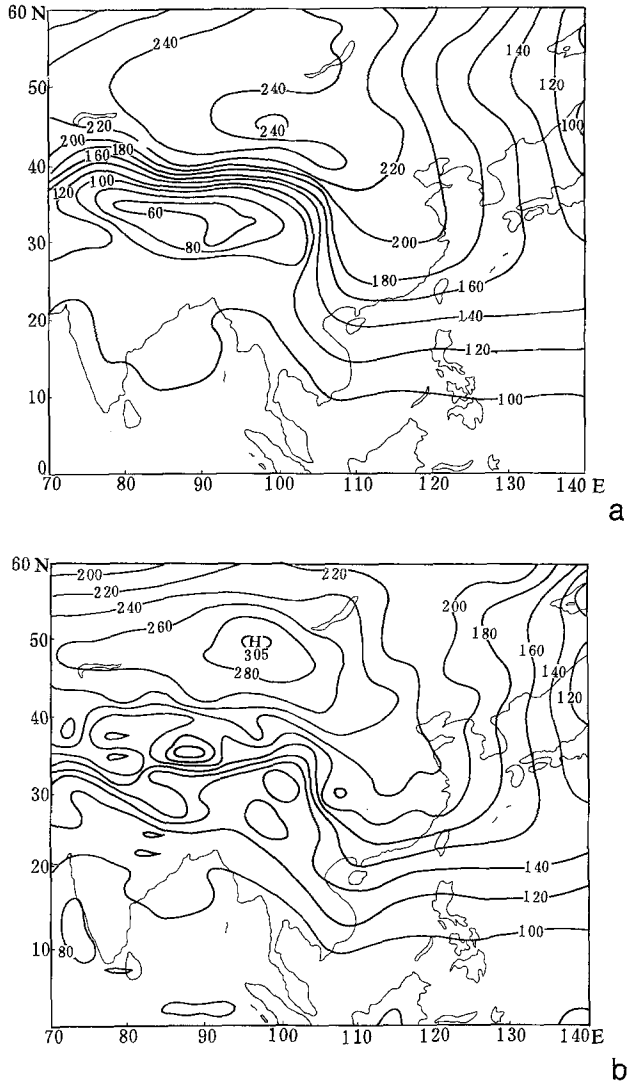

Fig. 12. The mean weather charts of 1 000 hPa. (a) for the winter for 1979–1980, and (b) for the winter fo 1983–1984. Unit: gm

branches, with the warm air advected over southern China by the southwesterly airflow in advance of the semi-permanent trough in the southern branch of westerlies to the south of the Tibetan Plateau. This may be used to explain why the cold surge is mainly confined in the layer below 700 hPa.

The association between the behavior of Siberian high and the cold surge may be more clearly seen through a contrasting study of winters of active cold surge and inactive cold surge. The winter of 1979/1980 was chosen as a year of inactive cold surge while the winter of 1983/1984 was considered as an active cold surge. The comparison of the occurrence frequency of cold surges for these two winters shows (Fig. 11) that the most significant difference showed up in distributions over the South China Sea. At 1 000 hPa, the frequency of occurrence of cold surge for the winter of 1983/1984 was one time higher than that for the winter of 1979/1980 (80%: 40%). At 850 hPa, the cold surge over the South China Sea for 1979/1980 winter was not detectable, and it only can be seen over the near-equatorial region of Indonesia and Malaysia. On the other hand, for the winter of 1983/1984, the cold surge over the central and southern part of the South China Sea was still very significant. At 700 hPa (not shown), the

cold surge for the winter of 1983/1984 still had a region of high frequency in Indonesia while the cold surge for the winter of 1979/1980 basically disappeared. Therefore, the above comparison indicates that the frequency of activity of cold surge over the South China Sea for the winter of 1983/1984 was higher and extended upward to higher level (700 hPa). In relation to these difference in cold surge, it is very interesting to compare the intensity of the Siberian highs for these two winters (Fig. 12). The intensity of the center of the cold high for the winter of 1983/1984 was 305 gm, while that for the winter of 179/1980 was only 240 gm, thus producing the pressure gradinets of different intensity over southern China and the South China Sea. The mean pressure gradient for the winter of 1983/1984 was greater than that for the winter of 1979/1980. This difference in the pressure gradient may be one factor responsible for the considerable difference in cold surge for these two winters. Therefore, the study of the build-up, outbreaks and southward propagation of the Siberian high is very important for better understanding of the development of cold surge in East Asia.

7. Conclusion

The present paper has addressed build-up, air mass transformation and propagation of the Siberian high and its relations to the development of cold surge in East Asia. The following conclusions have been drawn:

(i) The genesis and development of the Siberian high result from the combined effects of the mass convergence at middle and upper-level and the advection of the negative vorticity, as well as local thermal cooling. Long-wave radiative cooling in deep layer of the troposphere is a major component of local thermal factors which may cause the significant, compensating downward motion, thus leading to increase in mass convergence at upper-level. Heating in the upper troposphere due to subgrid-scale sensible heat transfer may be another important factor in creation and maintenance of mass convergence at upper level, through enhancement of the warm upper tropospheric anticyclone lying over the Siberian high.

(ii) Based on the direct estimate of sensible heat flux and latent heat flux from the surface by use of the similarity theory, the total heat flux is about 84 W/m^2 (northern China) or 75 W/m^2 (the eastern China). These magnitudes amount to one third of those over the warm ocean. The air mass transformation of the Siberian high over land is mainly caused by these heat fluxes from the underlying surface with the maximum of upward heat flux found in the afternoon of the day.

(iii) The Siberian high and its associated cold air outbreaks usually show a marked low-frequency meridional movement (southeastward propagation) with the period of 10–20 days. This low-frequency mode of the propagation of cold air outbreaks actually is a manifestation of low-frequency oscillation systems at middle and high latitudes and their effect on the circulation features at low-latitude.

(iv) The cold surge in East Asia and Southeast Asia is shallow, mainly confined in layer below 700 hPa. There are two major regions of cold surge: the East China Sea and the South China Sea, and the western Pacific to east of the Philippine islands. The activity of cold surge in these two regions is closely related to the intensity of the Siberian high and semi-permanent Indo-Burmese trough. The active cold surges occur when the Siberian high is unusually strong and the Indo-Burmese trough relatively weak.

Acknowledgements

I wish to convey my thanks to Dr. T. N. Krishnamurti for soliciting contributions from me. I am indebted to Messrs. Wen Shigen and Li Yunjin for their much help, and Miss Chao Qingchen for typing.

References

Bodurtha, F. T., 1952: An investigation of an anticyclogenesis in Alaska. *J. Meteor.*, **9**, 118–125.

Businger, J. A., Wyngaard, J. C., Izumi, Y., Bradley, E. F., 1971: Flux profile relationship in the atmospheric surface layer. *J. Atmos. Sci.*, **28**, 181–189.

Chang, C. P., Lau, K. M., 1980: Northeasterly cold surges and near equatorial disturbances over the winter MONEX area during December 1974. Part II: Planetary scale aspect. *Mon. Wea. Rev.*, **108**, 298–312.

Dallavalle, J. P., Bosart, L. F., 1975: A synoptic investigation of anticyclones accompanying North American polar air outbreaks. *Mon. Wea. Rev.*, **103**, 941–957.

Ding, Yihui, Krishnamurti, T. N., 1987. Heat budget of the Siberian high and the winter monsoon. *Mon. Wea. Rev.*, **115**, 2428–2449.

Krishnamurti, T. N., Gadgil, S., 1985: On the structure of the 30 to 50 day mode over the globe during FGGE. *Tellus*, **37 A**, 336–360.

Lau, K. M., 1982: Equatorial response to northeasterly cold surges as inferred from satellite cloud imagery. *Mon. Wea. Rev.*, **110**, 1306–1313.

Lau, N. C., Lau, K. M., 1984: The structure and energetics of midlatitude disturbances accompanying cold air outbreaks over East Asia. *Mon. Wea. Rev.*, **112**, 1309–1327.

Lim, H., Chang, C. P., 1981: A theory of midlatitude forcing of tropical motion during the winter motion. *J. Atmos. Sci.*, **38**, 2377–2392.

Louis, J. F., 1979: A parametric model of vertical eddy fluxes in the atmosphere. *Bound. Layer Meteor.*, **17**, 187–202.

Ninomiya, K., 1975: Large-scale aspects of air mass transformation over the East China Sea during AMTEX '74. *J. Meteor. Soc. Japan*, **53**, 285–303.

Ninomiya, K., 1977: Heat budget of the polar air mass transformation over Kuroshio region under the situation of strong subsidence. *J. Meteor. Soc. Japan*, **55**, 431–441.

Nita, T. S., So, S. S., 1980: Structure and heat, moisture and momentum budgets of a convective mixed layer during AMTEX '75. *J. Meteor. Soc. Japan*, **58**, 378–393.

Pan, H.-L., Zhou, F. X., 1985: The 10–20 day tropical-midlatitude interaction during winter monsoon season. *J. Meteor. Soc. Japan.*, **63**, 829–843.

Yang, D., Krishnamurti, T. N., 1981: Potential vorticity of monsoonal low-level flow. *J. Atmos. Sci.*, **38**, 2676–2695.

Author's address: Ding Yihui, Academy of Meteorological Science, State Meteorological Administration, Beijing, P. R. China.